International Research Journal of Engineering and Technology (IRJET) e-ISSN: 2395-0056
Volume: 09 Issue: 07 | July 2022 www.irjet.net p-ISSN: 2395-0072

METHOD FOR OPTIMIZATION OF COMPOSITE SANDWICH STRUCTURE USING ARTIFICIAL NEURAL NETWORK.

Rahul Sanjay Autade

Student, dept. of Mechanical Engineering, Pimpri Chinchwad College Of Engineering, Maharashtra, India.

Abstract - *laminates are utilized in a variety of fields, including naval, aeronautics, automobiles, etc. The objective of the panel's design is to maximize flexural strength, energy absorption, and flexural rigidity while minimizing weight. However, finding the optimum configuration of layer thickness and core thickness requires extensive destructive testing. Using a neural network, this study established the relationship between the configuration of laminates, such as layer thickness, core thickness, weight with the flexural strength, and the flexural rigidity of laminates. For this study, training data is collected via finite element analysis (FEA) of three-point bending tests of laminates with varying core and layer thicknesses and then utilized to train a neural network. This FEA study of a three-point bending test is conducted using the academic software ANSYS. An artificial neural network is used to perform regression. After hyperparameter optimization, 256 points of ANSYS data are used to train an artificial neural network model with an accuracy of 95.29 percent for deflection prediction and 95.05 percent for force prediction. This will decrease the amount of computation required to determine the optimal configuration after the neural network is trained.*

***Key Words*: composites sandwich, carbon fibre, artificial neural network, multi-objective optimization, design optimization.**

1.INTRODUCTION

Sandwich structures consist of a thin, high-strength outer layer and a low-strength inner core similar to the I-beam structure. It provides greater bending strength and stiffness with less weight. Sandwich structures are utilized in a variety of applications, including aircraft wings[1] , electric vehicles [2], monocoque structures, rooftops[3], and bridges[4] . For fibre reinforced composite sandwich panel manufacturing carbon fibre, glass fibre, Kevlar fibre, and natural fibres are used with PVC foam, balsa wood, and aluminium honeycomb core. In this analysis, carbon fibre and aluminium honeycomb structures are studied.

Face wrinkling, core shear, and face yielding, Intra-cell buckling, as well as the face indentation[5], are the primary failure modes of a sandwich panel in three-point bending. A three-point bending test is used to analyse sandwich panel for the above criteria. Failure mode must be determined in order to determine the weakest link in a sandwich structure. By reinforcing the weakest link, the overall panel strength can be increased. For the prediction of failure mode, researchers drew failure maps[6] based on large sample testing; however, these failure maps vary for different materials, and determining their boundaries requires a large number of sample tests.

In addition, these maps do not account for the panel weight parameter. The 3-point bending test of CFRP with an aluminium core is studied using the pre-post module and the inbuilt material library in the ANSYS student edition. Maximum failure stress can be determined using Maximum principal stress, maximum principal strain, tsai wu [7], tsai hill [8], and Hoffman theory [9]. Failure load and failure modes can be determined using inverse reserve factor (IRF) [10] in ANSYS. The dimensions of the monocoque construction of the test rig are fixed in formula student[11].

This type of intricate structure necessitates a great deal of computer power, and the outcomes vary depending on the production procedure. To circumvent this, an artificial neural network (ANN) is implemented to forecast sandwich structure attributes.

ANN is preferred to linear regression for prediction due to its superior performance[12], [13]. ANN is motivated by biological neural network[14]. Applications of ANN linear regression includes diesel pollution prediction[15], GDP growth prediction[16], stock market prediction[17], and computer vision[18]. Afterward, acquired data from ANSYS is utilised to train a model of an artificial neural network. With feed-forward architecture, a small number of hidden layers is sufficient to create multivariate polynomial regression for the model. Finally, the prediction with 95.45% accuracy is achieved.

2.PROBLEM DEFINITION

2.1 Material characteristics of the sandwich panel

With a fibre-to-resin ratio of 60:40, carbon fibre is chosen as the reinforcing fibre and epoxy resin as the matrix[10]. The composite properties Pc are generated from the individual fibre and matrix properties Pf and Pm, respectively.

$$P_c = X_f.P_f + X_m.P_m$$

Where X_f and X_m indicate the fibre volume fraction and matrix volume fraction in composite, respectively, while the suffixes 'f', 'm', 'c', and 's' stand for fibre, matrix, composite,

and sandwich, respectively. Because fibres are braided in the 0±90 direction, the resulting characteristics are Pc/2

Consider the plane of weaving to be XY. Young's modulus (E) of CFRP in the direction of the weaving pattern (x and y) is 61.34 GPa. Poisson's ratio (v) is 0.04 in the xy plane and 0.30 in the yz, xz plane. Shear modulus (G) in the xy plane is 3,3 GPa, while in the yz and xz planes, it is 2.7 GPa. To the x and y directions Tensile stress limit is 805 MPa and compression stress limit is 509 MPa. In the xy plane, the shear stress limit is 125 MPa, but in the yz and xz planes, it is 65 MPa.

Then, six types of honeycomb cores with varying layer thickness and core thickness were selected. The following are the characteristics of this honeycomb core[19].

Table -1: Honeycombs with different properties for different foil gauge and cell size.

Sr.no	Foil Gauge(mm)	Ecz	Gyz	Gxz
1	0.0254	137.9	75.842	144.79
2	0.0381	310.26	111.7	220.63
3	0.0508	482.63	146.17	296.47
4	0.0635	723.95	179.26	379.21
5	0.0762	930.79	199.95	448.16
6	0.1016	1379	253.736	592.97
Sr.no	σ_{cz}	τ_{yz}	τ_{xz}	ρ
1	0.655	0.344	0.586	25.63
2	1.379	0.551	0.930	36.842
3	2.1374	0.861	1.379	48.055
4	2.8269	1.103	1.723	59.268
5	3.8611	1.379	2.137	67.278
6	5.5158	1.930	2.964	86.5

2.2 Bending test constrains

The dimensions of the panel are 500 mm in length (L), 400 mm between supports (l), and 275 mm in width (b). Round load applicators with a radius of 50 mm were used. This test rig constrains were chosen from formula student testing standards[11].

The sort of contact between the load applicator and sandwich panel is frictionless. Core thickness is c, layer thickness is t, and distance between CFRP centre planes is d. h is the sandwich panel's thickness.

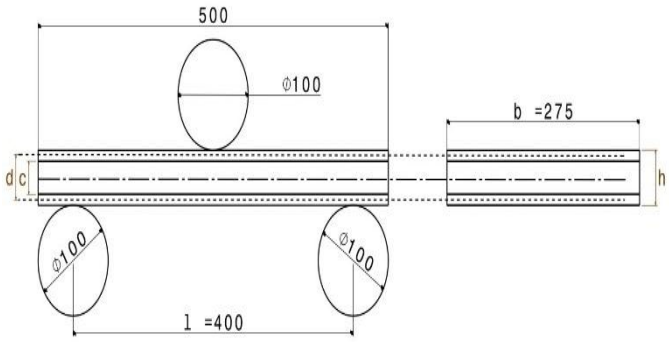

Fig -1: Constrains used in 3-Point bending test

2.3 Maximization of load capacity, stiffness and minimization of weight

The purpose of a composite panel is to reduce the weight of panel(W) for a specific three-point bending load (P) application.

As a result of the imposed load, stresses develop in the upper and lower layers. This layer's stress is proportional to the applied load on the sandwich. However, if the failure in the sandwich layer happens due to core shear, core buckling, or face wrinkling, then the failure occurs before the laminate top layers reach their ultimate yield strength. Similar to how the weakest link in a chain dictates the strength of a laminate. Because of this, it is necessary to maximise the stress in the CFRP layer while minimising its weight. For weight consideration, the surface density of the layer must be taken into account, assuming that the dimensions of the test rig and the dimensional constraints for a specific component remain constant. Therefore, the optimization problem can be defined as

Maximization… F/d, U.

Minimization… W.

3 Mathematical model

For optimization, we must determine bending stiffness (D), energy absorption (U), and Surface Density (S), which depend on the material's properties and dimensions. Surface density of sandwich panel can be calculated by combining surface density of composite layer and its core.

$$S = \rho_s . h = \rho_f t + \rho_c c$$

3.1 Beam Theory

To prevent edge loading during a three-point bending test, the sandwich material is kept overhanging by 50mm. The stiffness of a sandwich panel in a three-point bend is determined by following equation.

$$D = \frac{E_f b t^3}{6} + \frac{E_f b t d^2}{2} + \frac{E_c b c^3}{12}$$

Thickness of CFRP is very small therefore second term in equation makes insignificant contribution in total stiffness. E_c is young's modulus of core is small compared to young's modulus of CFRP. So, the resultant panel stiffness is…

$$D = E_f \frac{b t d^2}{2}$$

Therefore, maximum stress developed for the bending moment M in the midpoint of 3-point bending test stress developed in ply is…

$$\sigma_f = \frac{M E_f d}{2D} = \frac{WL}{4dt}$$

However, this equation neglects shear effect of core material, which is significant for low density materials.
This stress can be calculated by finite element analysis (FEA). Stress developed in CFRP ply is directly proportional to the applied load. 1KN load is applied on each iteration therefore failure load can be calculated by using largest inverse reserve factor as follows

$$F_{\max} = \frac{1KN}{IRF}$$

Failure stress can be calculated by multiplying failure load with stress at 1KN load.

$$\sigma_{\max} = \sigma \times F_{\max}$$

3.2 Failure theories in composites.
To determine energy absorption by panel we have to determine failure force and displacement x at that force as.

$$U = \int_0^x F . dx$$

This failure force is determined in FEA by using deferent failure theories. Some of the relevant failure theories are applied for this analysis which are as follows[10].
Maximum Principal Strain Criterion: This theory is for isotropic mechanics of materials. The maximum strain in principle plane should be less than failure strain of material to avoid failure by this principle. Principle strain is given by

$$\varepsilon = \frac{1}{E}\left\{\frac{(1-\vartheta)(\sigma_1+\sigma_2)}{2} \pm (1+\vartheta) \times \sqrt{\left(\frac{(\sigma_1+\sigma_2)}{2}\right)^2 + \tau_{12}^2}\right\}$$

Were…

$$\sigma_1 = F_{1t} \text{ if } \varepsilon_1 > 0; \sigma_1 = F_{1t} \text{ if } \varepsilon_1 > 0$$

$$\sigma_1 = -F_{1c} \text{ if } \varepsilon_1 < 0; \sigma_1 = -F_{1c} \text{ if } \varepsilon_1 < 0$$

Maximum Principal Stress Criterion: Principal stress in the ply should be less than failure stress of ply. Principal stress in isotropic ply is

$$\sigma = \frac{(\sigma_1+\sigma_2)}{2} \pm \sqrt{\left(\frac{(\sigma_1+\sigma_2)}{2}\right)^2 + \tau_{12}^2}$$

Were…

$$\sigma_1 = F_{1t} \text{ if } \sigma_1 > 0; \sigma_1 = F_{1t} \text{ if } \sigma_1 > 0$$

$$\sigma_1 = -F_{1c} \text{ if } \sigma_1 < 0; \sigma_1 = -F_{1c} \text{ if } \sigma_1 < 0$$

Tsai-Wu Failure Criterion:
Tension and compression in the composite layers are taken into consideration in the Tsai-Wu failure criteria. The criteria are given by the following equation.

$$f = \frac{\sigma_1^2}{X_t X_c} + \frac{\sigma_2^2}{Y_t Y_c} + \frac{\tau_{23}^2}{Q^2} + \frac{\tau_{13}^2}{R^2} + \frac{\tau_{12}^2}{S^2} + \left(\frac{1}{X_t} - \frac{1}{X_c}\right)\sigma_1 + \left(\frac{1}{Y_t} - \frac{1}{Y_c}\right)\sigma_2 + 2F_{12}\sigma_1\sigma_2$$

Tsai-Hill Failure Criterion:
Tsai-Hill failure theory is based on the Von-Mises failure criteria for isotropic material. Failure of CFRP is occurred if following force is exceeded [20].

$$f = \left(\frac{\sigma_1}{X}\right)^2 + \left(\frac{\sigma_2}{Y}\right)^2 + \left(\frac{\tau_{23}}{Q}\right)^2 + \left(\frac{\tau_{13}}{R}\right)^2 + \left(\frac{\tau_{12}}{S}\right)^2 - \frac{\sigma_1\sigma_2}{X^2}$$

4. FINITE ELEMENT ANALYSIS (FEA)

4. 1) Geometry in CATIA V5

For doing finite element analysis of 3-point bending test, first of all geometry is built in CATIA V5. In this geometry supporters are of 50 mm radii and 400 mm apart with load applicator in the middle of the same size. Instead of putting solid sandwich only surface of 275 mm × 500 mm is made over supporters so, in the ANSYS lamination of required material with particular thickness can be stacked.

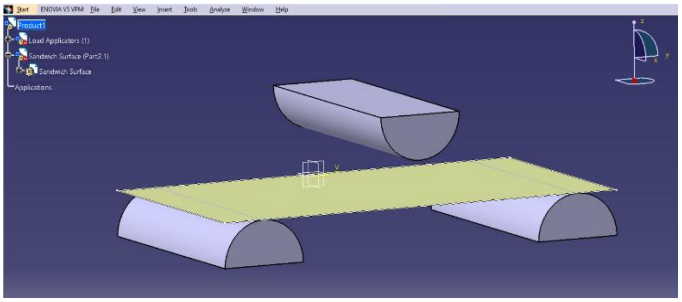

Fig-2: Geometry in CATIA V5

4.2) Modelling and Meshing

Load applicators and surface are imported in separate module Because surface needs to be stacked up with CFRP and honeycomb in ACP (pre) module. Afterwards the were combine in 'static structure' module.

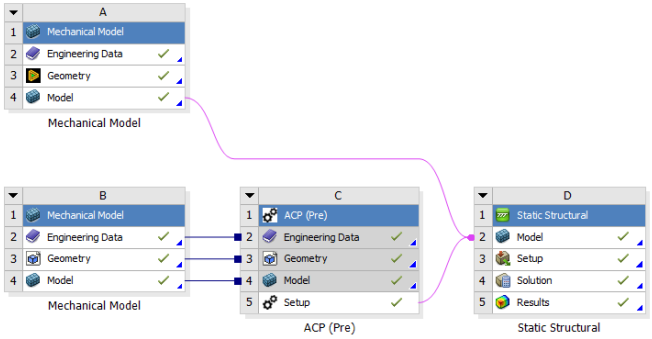

Fig-3: Modelling tree in ANSYS.

Course meshing is done on load applicator as stress analysis on load applicator is not required. On the other hand, meshing on sandwich panel is fine to analyze more accurately.

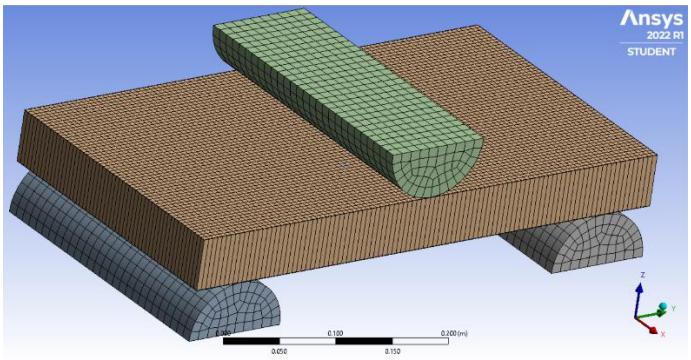

Fig-4: Meshing in ANSYS.

4.3 ACP (pre)

In ACP (pre) stacking of CFRP and honeycomb is done as shown in fig-5. Pail green and green arrow shows fiber direction, purple arrows indicate direction of staking. This stacking is iterated over different layer thickness and core thickness as mentioned in below tables.

Table -2: Iterations of layer thickness.

Sr.no	1	2	3	4	5	6
t(mm)	0.28	0.56	0.84	1.12	1.68	2.24

Table -3: Iterations of core thickness.

Sr.no	1	2	3	4	5	6	7
d(mm)	40	30	28	18	14	12	10

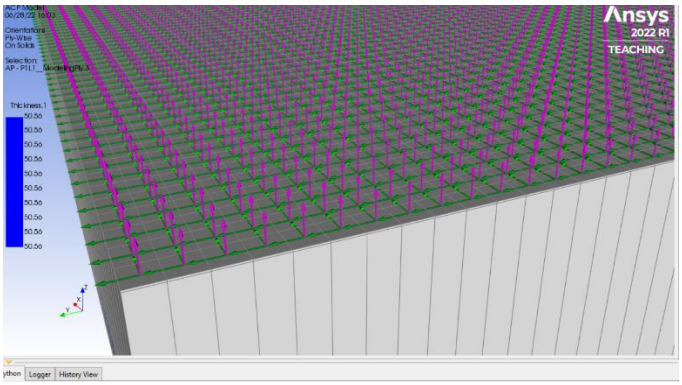

Fig-5: Fiber direction and ply orientation direction.

4.4 Static structure

First of all, in static structure constrains are applied. Force on a load applicator of 1000 N force in downward direction and on supporters as fixed support are applied. Because of applied load maximum directional deformation (δ) forms at centre of panel which is used to find out stiffness of panel.

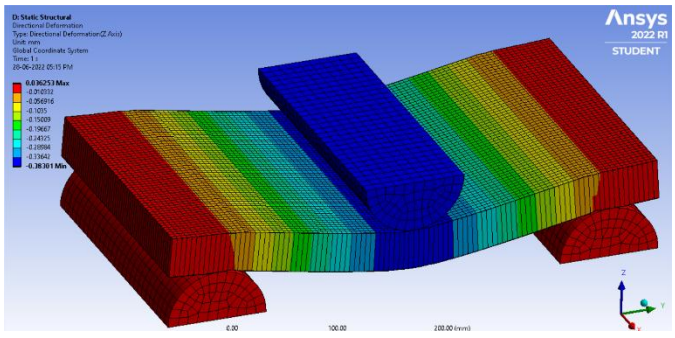

Fig-6: Z directional deformation.

Finally, by applying sandwich failure criteria CIRF and WIRF is determined to calculate failure force from equation.

$$F_{\max} = \frac{1KN}{IRF}$$

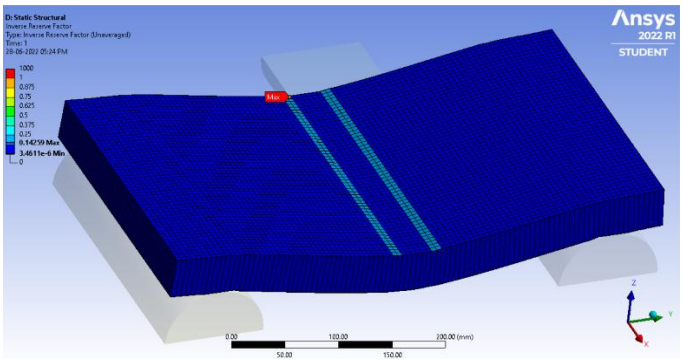

Fig-7: Core failure criteria (CIRF).

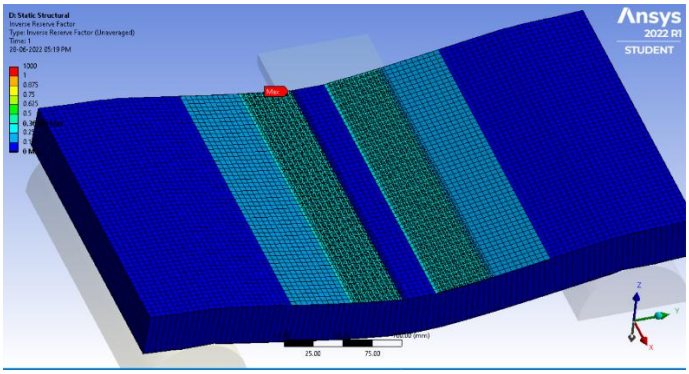

Fig-8: Face wrinkling failure criteria (WIRF).

5. Artificial Neural Network (ANN)

ANN is inspired by human brain neurons and their network. Perceptron is mathematical model of single biological neuron. By arranging these perceptions in neural network architecture any mathematically complex function can be formed. Single k^{th} neuron with x input can mathematically describe as.

$$u_k = \sum_{j=1}^{m} w_{kj} x_j$$

$$y_k = \varphi(u_k + b_k)$$

w_{kj} is weight which is represent power of particular neutron to get activated. These weights get updated in every data pass from neurons. Bias is represented by b_k in equation. φ in equation is activation function which introduces nonlinearity in ANN model.

5. 1) Model

The inputs for the ANN include all sandwich pane properties that are relevant to our optimization problem. The ANN's output consists of all failure properties. For this multivariate polynomial regression problem feed forward neural network model is used[12].

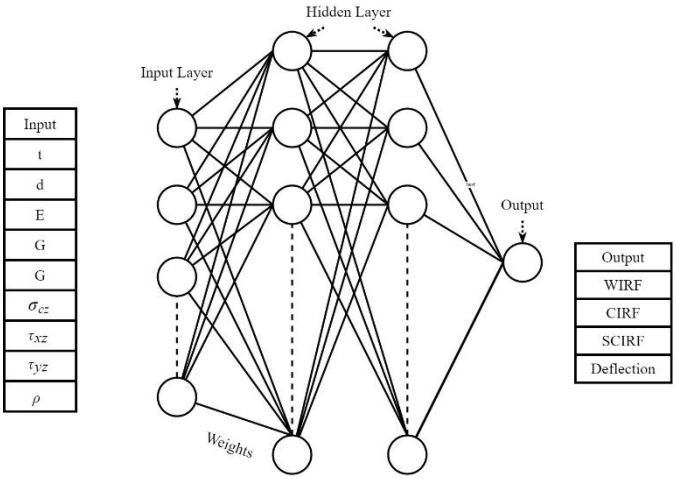

Fig-9: Artificial Neural Network model.

First of all, the data from different iteration from ANSYS is collected. This data is split into 70:15:15 to perform training, validation and testing respectively. Because of WRIP, SCIRP and CIRP and deflection are independent of each other separate model were built for each parameter prediction.

5.2) Over fitting in ANN model

Epoch is how many times same data point pass through neural network. As this data point pass over and over again mean absolute error (MAE) is get reduced. However, if after curve fitting training of neural network is not stopped the MAE is increases with epochs. This is result of over fitting of curve.

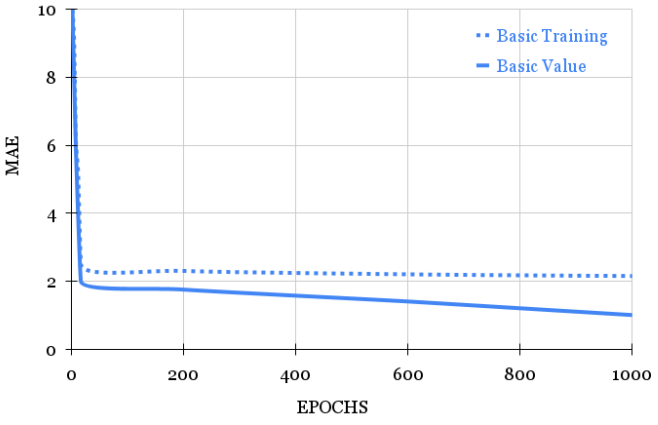

Chart -1: Mean absolute error without early stop.

This problem is solved by early stopping of training. Therefore, model training is terminated if the error of cost value, which is the difference between the true value and the predicted value of validation data, increases rather than decreases during training.

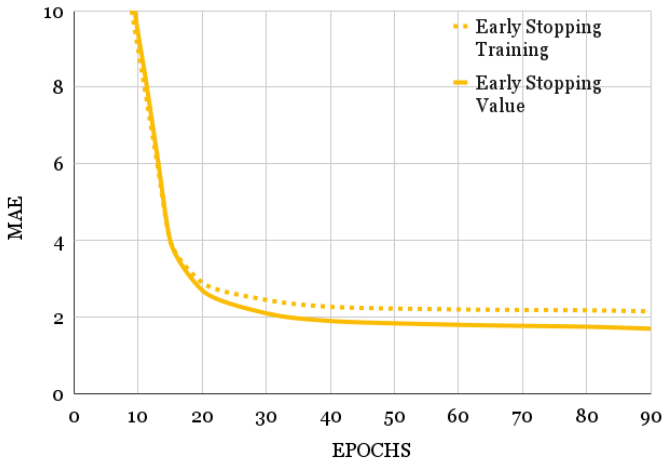

Chart -2: Mean absolute error with early stop.

5.3) Hyper-parameters optimization In the ANN model

The hyper-parameters for the ANN are number of neurons in hidden layer, number of hidden layers, activation function, initial seed, learning rate. These hyperparameters decide performance of model. Selection of hyper-parameter is done by running model with each possible configuration and selecting which gives least mean absolute error (MAE) with validation data. Iterated hyper-parameters are as following.

Table -4: Hyper-parameters over which ANN is iterated

Hyper-parameter	Iterations
Number of neurons hidden layer	32+n.64 where n is from 0 to 14
Number of hidden layers	1,2,3
Activation function	relu, tanh, softmax, selu, softsign, hard_sigmoid, exponential, softplus, elu, sigmoid, LeakyReLU(alpha=0.3)
Initial seed	2+m4 where m is from 0 to 14
Learning rate	0.001, 0.0001

6. Results and Discussion

Models for deflection, force, CIRF, SCIRF and WIRF are iterated for hyper-parameters from table-4. Then after least error hyper parameter were choose for prediction. Those parameters and there corresponding errors are listed in table below.

Table -5: Least error hyper-parameters and MAE

Hyperparameter	Deflection	Force	CRIF	WIRF
Number of neurons in hidden layer	32	32	32	160
Number of hidden layers	4	2	4	2
Activation function	softplus	tanh	softmax	softmax
Initial seed	18	38	62	46
Learning rate	0.001	0.001	0.001	0.001
MAE of validation data	0.0023%	0.710%	0.0064%	0.0042%
MAE of prediction of test data	4.71%	4.95%	9.44%	4.55%

7) Conclusion

In this study, prediction of failure force and deflection of different configuration composite sandwich structure is done by using artificial neural network. This model configuration for force gives 95.05% and for deflection it gives 95.29% of accuracy. From these predicted data, sandwich configurations that are more optimal can be chosen without FEA, thereby reducing computational time. On a Ryzen 5 machine, approximately one month of computational time was required. 99 percent of this method's time was devoted to iteratively finding the hyperparameters. By selecting hidden layers, number of neurons and learning rate manually, computational time through this method can be significantly reduced. With additional training data, the model's accuracy can be improved.

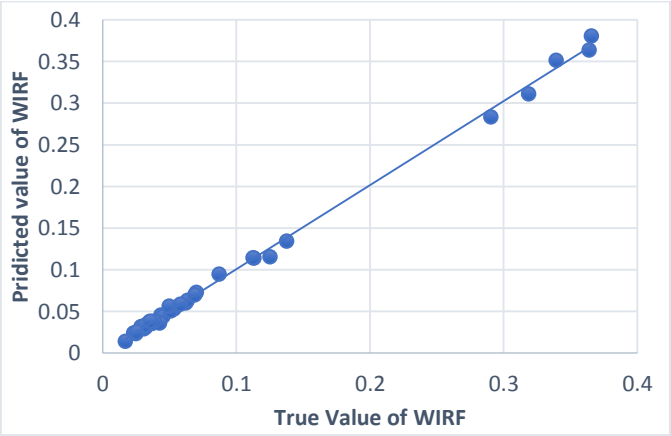

Chart -3: Scatter plot of true vs predicted value.

Table -3: Hyper-parameters over which ANN is iterated

Sr. No	Sample No	Deflection test	Deflection predictions	Force test	Force predictions	CIRF test	CIRF predictions	WIRF test	WIRF predictions
1	178	0.8051	0.7723	7.3806	8.1149	0.1354	0.1823	0.0604	0.0621
2	153	0.1583	0.1576	38.8636	28.063	0.0257	0.1062	0.0242	0.0232
3	106	0.2633	0.2696	8.8636	7.1023	0.1128	0.1724	0.0543	0.0534
4	111	0.1984	0.2076	31.3646	25.2302	0.0318	0.1162	0.0318	0.0286
5	125	0.4858	0.524	19.4306	14.8641	0.0514	0.1402	0.0514	0.0496
6	225	0.6162	0.6012	4.0492	5.9559	0.2469	0.287	0.0457	0.0435
7	122	0.525	0.5068	10.6489	8.8077	0.0939	0.1573	0.0529	0.0532
8	214	0.287	0.283	14.2233	16.6136	0.0703	0.1098	0.0293	0.0307
9	45	4.1065	4.0536	3.2141	3.8888	0.2668	0.2578	0.3111	0.3187
10	194	0.0802	0.0992	42.2904	37.4265	0.0236	0.0942	0.014	0.017
11	118	0.272	0.2838	26.8398	20.7584	0.0372	0.1226	0.0372	0.0346
12	176	0.8843	0.868	3.7397	4.0789	0.2674	0.314	0.0634	0.0634
13	217	0.5767	0.5465	2.9222	4.2463	0.3422	0.3553	0.0443	0.0451
14	101	0.1419	0.1584	23.2801	19.6407	0.0429	0.0902	0.031	0.0323
15	173	0.5908	0.5955	14.7551	14.3325	0.0677	0.1223	0.0505	0.051
16	154	0.3462	0.3258	4.7319	4.3934	0.2113	0.2674	0.0565	0.0498
17	180	0.7667	0.7701	12.6491	13.1196	0.079	0.1315	0.0589	0.0581
18	108	0.2239	0.2254	17.6401	14.1594	0.0566	0.1059	0.0356	0.0373
19	184	1.1193	1.069	4.8966	5.618	0.2042	0.2535	0.0731	0.07
20	8	0.5478	0.5644	3.5289	5.1327	0.1205	0.1946	0.2833	0.2905
21	55	0.1638	0.1909	27.7138	31.6978	0.0353	0.125	0.036	0.0426
22	90	1.4619	1.5628	8.7496	8.0754	0.1142	0.1912	0.1142	0.1133
23	89	1.4775	1.5483	8.7275	8.9748	0.1145	0.1731	0.1145	0.1125
24	5	0.2845	0.3002	8.6408	25.8743	0.0667	0.1059	0.1157	0.1252
25	22	1.3725	1.3535	2.7487	2.8919	0.2024	0.3014	0.3638	0.364
26	37	2.8383	2.8131	2.8464	3.2883	0.2211	0.291	0.3513	0.3394
27	156	0.2607	0.2581	11.7105	10.1767	0.0853	0.1459	0.0315	0.0313
28	12	0.4869	0.4961	7.4299	18.3281	0.0904	0.1173	0.1345	0.1376
29	109	0.2172	0.2163	22.0337	17.1056	0.0453	0.0993	0.0329	0.031
30	135	1.4742	1.4092	4.7078	4.6039	0.2124	0.2703	0.0948	0.0871
31	219	0.4562	0.4583	7.1664	9.3052	0.1395	0.1976	0.0384	0.0388
32	116	0.2939	0.2858	18.3968	14.273	0.0543	0.1112	0.0382	0.0357
33	205	0.1978	0.2284	12.1738	13.4131	0.0821	0.1369	0.0235	0.0249
34	204	0.2238	0.2579	7.793	9.3948	0.1283	0.1843	0.0252	0.0253
35	44	4.1494	4.1862	2.6263	2.9456	0.2833	0.312	0.3807	0.3656
36	188	1.025	1.0141	12.9329	11.4191	0.0773	0.1483	0.0698	0.069

8. Reference

[1] O. Dababneh, T. Kipouros, and J. F. Whidborne, "Application of an efficient gradient-based optimization strategy for aircraft wing structures," *Aerospace*, vol. 5, no. 1, Mar. 2018, doi: 10.3390/aerospace5010003.

[2] Y. Xiao *et al.*, "The Bending Responses of Sandwich Panels with Aluminium Honeycomb Core and CFRP Skins Used in Electric Vehicle Body," *Advances in Materials Science and Engineering*, vol. 2018, 2018, doi: 10.1155/2018/5750607.

[3] J. J. del Coz Díaz, P. J. García Nieto, F. P. Álvarez Rabanal, and C. Betegón Biempica, "Finite element analysis of thin-walled composite two-span wood-based loadbearing stressed skin roof panels and experimental validation," *Thin-Walled Structures*, vol. 46, no. 3, pp. 276–289, Mar. 2008, doi: 10.1016/j.tws.2007.07.020.

[4] Agusril, N. M. Nor, and A. M. A. Zaidi, "Failure analysis of Carbon Fiber Reinforced Polymer (CFRP) bridge using composite material failure theories," in *Advanced Materials Research*, 2012, vol. 488–489, pp. 525–529. doi: 10.4028/www.scientific.net/AMR.488-489.525.

[5] J. Xiong *et al.*, "Mechanical behaviors of carbon fiber composite sandwich columns with three dimensional honeycomb cores under in-plane compression," *Composites Part B: Engineering*, vol. 60, pp. 350–358, Apr. 2014, doi: 10.1016/j.compositesb.2013.12.049.

[6] A. Petras, "Design of Sandwich Structures," 1998. pp. 4-8.

[7] S. W. Tsai, W.-P. Afb, E. M. Wu, and S. Louis, "A General Theory of Strength for Anisotropic Materials." Pp. 58-80, 1971.

[8] J. Aboudi and B. Bednarcyk, "Tsai-Hill Criterion Failure criteria and margins of safety."

[9] O. Hoffman, "The Brittle Strength of Orthotropic Materials," *Journal of Composite Materials*, vol. 1, no. 2, pp. 200–206, Apr. 1967, doi: 10.1177/002199836700100210.

[10] "ANSYS Composite PrepPost User's Guide," 2013. [Online]. Available: http://www.ansys.com

[11] "FS-Rules_2022_v1.0".

[12] K.-Y. Lee *et al.*, "Comparison and Analysis of Linear Regression & Artificial Neural Network," 2017. [Online]. Available: http://www.ripublication.com

[13] E. Tosun, K. Aydin, and M. Bilgili, "Comparison of linear regression and artificial neural network model of a diesel engine fueled with biodiesel-alcohol mixtures," *Alexandria Engineering Journal*, vol. 55, no. 4, pp. 3081–3089, Dec. 2016, doi: 10.1016/j.aej.2016.08.011.

[14] I. Goodfellow, Y. Bengio, and A. Courville, "Deep Learning."

[15] R. J. Atkinson and C. M. Atkinson, "Neural network-based diesel engine emissions prediction using in-cylinder combustion pressure Machine Learning for Engine and Powertrain Control and Calibration View project HEV Development View project," 2012. [Online]. Available: https://www.researchgate.net/publication/313192543

[16] M. Jahn, "Artificial neural network regression models: Predicting GDP growth." [Online]. Available: www.hwwi.org

[17] R. G. Ahangar, M. Yahyazadehfar, and H. Pournaghshband, "The Comparison of Methods Artificial Neural Network with Linear Regression Using Specific Variables for Prediction Stock Price in Tehran Stock Exchange." [Online]. Available: http://sites.google.com/site/ijcsis/

[18] S. Lathuilière, P. Mesejo, X. Alameda-Pineda, and R. Horaud, "A Comprehensive Analysis of Deep Regression," Mar. 2018, doi: 10.1109/TPAMI.2019.2910523.

[19] "HexWeb ™ Honeycomb Attributes and Properties."

[20] S. N. Alnomani, M. B. Hunain, and S. H. Alhumairee, "INVESTIGATION OF DIFFERENT FAILURE THEORIES FOR A LAMINA OF CARBON FIBER/EPOXY MATRIX COMPOSITE MATERIALS," 2020.